

## Semi-automatic Prostate Segmentation via a Hidden Markov Model with Anatomical and Textural Priors

Christian Scharfenberger<sup>1</sup>, Dorothy Lui<sup>1</sup>, Farzad Khalvati<sup>2</sup>, Alexander Wong<sup>1</sup>, and Masoom Haider<sup>2,3</sup>

<sup>1</sup>Systems Design Engineering, University of Waterloo, Waterloo, Ontario, Canada, <sup>2</sup>Department of Medical Imaging, University of Toronto, Toronto, Ontario, Canada,

<sup>3</sup>Sunnybrook Health Sciences Centre, Toronto, Ontario, Canada

### Introduction

The contouring and segmentation of the prostate gland is an important task in prostate cancer screening using Magnetic Resonance Imaging (MRI), and essential for active surveillance, treatment planning and building patient models for preoperative planning [1]. However, the manual contouring and segmentation process can be tedious and subjective and requires extensive interpretation of each slice by an experienced professional. Computer-aided analysis can speed up the segmentation process while reducing subjectivity and maintaining accuracy. A major challenge of automatic prostate segmentation is the abundance of detailed textures around the prostate boundary. Semi-automatic methods such as [2, 3] utilize user-guidance to increase success rates by harnessing the doctor's expertise. Prostate segmentation approaches based on active contours [2, 3] have the potential for precise segmentation but pose a high risk of converging to local minima, making it susceptible to imprecise boundary detection in noisy and textured MR images. The proposed approach to semi-automatic prostate segmentation (SAE) uses anatomical priors and texture characteristics to guide the contour towards the prostate gland by leveraging user-guidance, texture, and anatomical characteristics.

### Materials and Methods

We propose a novel method for semi-automatic prostate segmentation based on active contours. In the active contours model [4] (Eq. 1), an energy minimizing curve (snake) is guided by external ( $E_{ext}$ ) and internal ( $E_{int}$ ) energies to extract a boundary of interest.

$$E_{Snake} = \int_0^1 E_{int}(v(s)) + E_{ext}(v(s)) ds \quad (1)$$

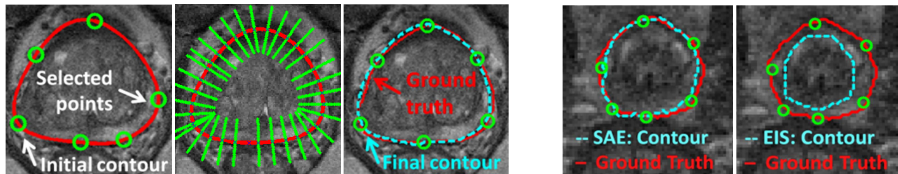
The classic snake model aims to minimize the snake energy but poses a high risk of converging to local minima while requiring an iterative implementation. A Decoupled Active Contours (DAC) model [4] overcomes this challenge with a faster converging iterative solution by optimizing the external and internal energies individually. The proposed approach uses a modified DAC framework to optimize the energy components in order to explicitly consider texture characteristics, the anatomical shape of the prostate gland and user input. First, the user selects points along the prostate contour to initialize a Hidden Markov Model (HMM) with trellises of size  $[-u_{inner}, u_{outer}]$ . The external energy of the HMM is then optimized by considering the transition probabilities  $p(z_j, z_{j+1})$  (Eq.2) from the current state  $z_j$  to its subsequent state  $z_{j+1}$ . The transition probability is based on the greatest similarity  $P(t_i^r | t_j^r) = \prod P(t_{i,k}^r, t_{j,k}^r)$  between a reference texture region  $t_i^r$  in  $z_j$  and each neighborhood  $t_j^r$  around a pixel  $k$  in the adjacent trellis at  $z_{j+1}$ . The similarity  $P(t_{i,k}^r, t_{j,k}^r)$  follows a Rician-likelihood (Eq. 3) to account for the Rician-distributed nature of MRI data.

$$p(z_j, z_{j+1}) = \begin{cases} P(t_i^r | t_j^r) & \text{if } z_j \in [-u_{inner}, u_{outer}] \\ 0 & \text{otherwise} \end{cases} \quad (2) \quad P(t_{i,k}^r, t_{j,k}^r) = \frac{|t_{i,k}^r - t_{j,k}^r|}{\sigma^2} \exp\left(\frac{-(|t_{i,k}^r - t_{j,k}^r|^2 + v^2)}{2\sigma^2}\right) I_0\left(\frac{|t_{i,k}^r - t_{j,k}^r|v}{\sigma^2}\right) \quad (3)$$

This transition probability guides the snake based on the assumption that the prostate will have consistent texture characteristics around its boundaries. It also considers a trellis around the user-guided snake to reinforce the probability of texture regions closer to the prostate interior over texture regions extending outside the contour. Subsequently, the internal energy is optimized using a weighted linear least squares and linear model to consider the relative smoothness of the prostate gland anatomy. Figure 1 provides an overview of the presented method. SAE was validated and compared against another user-guided active contour approach [3] based on MRI data of 10 patients (ages 58–80 years, median age of 69). The data were acquired with the local institutional research ethics board approval using a Philips Achieva 3.0T and resolution ranging from 1.36 x 1.36 mm<sup>2</sup> to 1.67 x 1.67 mm<sup>2</sup>, with a median of 1.56 x 1.56 mm<sup>2</sup>.

### Results and Discussion

To investigate the potential of our approach, we evaluated SAE based on MRI data from 10 patients by segmenting the apex, base, and mid-gland slices. These slices are good representatives of the prostate, with the apex and base slices considered as the two most difficult slices to segment. Medical experts segmented the prostate using SAE three times by selecting 4, 6, and 8 initial points. The result obtained were compared against ground-truths provided by an experienced radiologist based on Dice coefficient, Jaccard index, accuracy, sensitivity and specificity. Table 1 illustrates the results obtained for SAE based on 6 initial points. While 4 points are too few to segment the prostate gland properly, 8 points did not improve segmentation significantly, i.e., less than 1.0% for the tested metrics. Hence, 6 points were found to be beneficial in striking a balance between segmentation performance and time needed for point selection (7.36s for 6 points, 10.15s for 8 points). SAE was then evaluated against Enhanced Intelligent Scissors (EIS) [3]. Results show that SAE consistently outperforms EIS (Table 1) and indicate a clear improvement in prostate segmentation, with Fig. 2 showing the segmented prostate gland based on SAE and EIS[3]. In summary, the proposed approach to prostate gland segmentation has the potential for more reliable computer-aided analysis for physicians.



	SAE	EIS[3]
Dice	<b>91.4%, 3.1%</b>	80.7%, 9.1%
Jaccard	<b>84.3%, 5.1%</b>	68.5%, 11.9%
Accuracy	<b>99.8%, 0.1%</b>	99.6%, 0.2%
Sensitivity	<b>93.5%, 4.8%</b>	69.8%, 12.5%
Specificity	<b>99.8%, 0.9%</b>	99.3%, 0.1%

**Fig. 1:** Initial contour, trellis formation, and final contour. **Fig. 2:** Visual comparison of SAE and EIS[3]. **Tab.1:** Segmentation performance, 6 initial points.

### References

- [1] Maan *et al.*, "A new prostate segmentation approach using multispectral Magnetic Resonance Imaging and a statistical pattern classifier" SPIE, 2012
- [2] Zhang *et al.*, "Boundary Delineation in Prostate Imaging Using Active Contour Segmentation Method with Interactively Defined Object Regions", Prostate Cancer Imaging, LNCS 6367, pp. 131–142, 2010
- [3] Mishra *et al.*, "Improved Interactive Medical Image Segmentation using Enhanced Intelligent scissors", EMBC, 2008.
- [4] Lui *et al.*, "Enhanced Decoupled Active Contours Using Structural and Textural Variation Energy Functionals", IEEE TIP, vol.23, no.2, pp.855-869, 2014